SoRo

Soft Robotics

Open camera or QR reader and
scan code to access this article
and other resources online.

ORIGINAL ARTICLE

Exo-Glove Poly III: Grasp Assistance by Modulating Thumb and Finger Motion Sequence with a Single Actuator

Kyu Bum Kim,[1,2] Hyungmin Choi,[1,2] Byungchul Kim,[1–3,*] Brian Byunghyun Kang,[4] Sangheui Cheon,[1,2] and Kyu-Jin Cho[1,2]

Abstract

In daily living, people grasp an object through the steps of "pre-shaping" and "enclosing," with the thumb playing a crucial role with its multiple degrees of freedom. When assisting individuals with hand impairments using soft wearable robots, it is important to simplify the robot by reducing the number of actuators and to provide different grasping strategies based on various objects being handled. In this article, we propose a tendon-driven soft wearable hand robot, Exo-Glove Poly III, that uses a single actuator for assisting two types of grasping strategies for people with hand impairment. To move the thumb and other fingers with a single actuator, we developed a slack-based sequential mechanism that allows movements to occur at different timings by varying the initial slack lengths of each tendon. Based on our observations of grasping strategies and the proposed novel actuation system, a slack-based sequential actuator (318 g, including electronic circuits) was designed and integrated with the glove (90 g) using a commercial armband to make the system portable. The robotic system was evaluated by a healthy subject, showing how the thumb moves by the tendon routings and how the mechanism works for each grasping strategy.

Keywords: soft wearable robot, assistive device, tendon-driven mechanism, under-actuation mechanism

Introduction

Grasping plays a vital role in activities of daily living. It consists of two phases: pre-shaping, where the hand adjusts its posture according to the object, and enclosing, where the fingers apply force to grasp it.[1] During the pre-shaping phase, the size of the space for the object (hand aperture) increases until the object can fit within the aperture.[2]

Then in the enclosing phase, the size of the aperture gradually decreases as the fingers move toward the object until they make contact with it.

In both phases of grasping, the thumb plays a vital role with its multiple degrees of freedom (DOF) joints, allowing the thumb to move in a wide range of motions.[3] The joints coordinate to generate and combine the various thumb motions, like flexion/extension and abduction/adduction.[4,5]

---

[1]Biorobotics Laboratory, Department of Mechanical Engineering/Soft Robotics Research Center/IAMD, Seoul National University, Gwanak-gu, Korea.
[2]Institute of Engineering Research, Seoul National University, Gwanak-gu, Korea.
[3]Distributed Robotics Laboratory, Computer Science and Artificial Intelligence Laboratory, Massachusetts Institute of Technology, Cambridge, Massachusetts, USA.
[4]Department of Artificial Intelligence and Robotics, Sejong University, Seoul, South Korea.
*B.K. did this work at SNU.

Especially in the pre-shaping phase, the unique motion of the thumb, called the opposition, leads to the shape grasp posture.[6] This motion enables the thumb to be positioned in various ways relative to the other fingers to form the proper posture[7] and provides the basis for categorizing grasp postures into abducted and adducted thumb types.[8] In other words, strategies to grasp the object can be categorized according to the thumb opposition (Fig. 1).

Given the importance of the thumb's motion in grasping, various soft wearable hand robots have been developed to assist individuals with weakened or impaired thumb dexterity.[9] Researchers have explored various ways to assist thumb movements, including two-DOF mechanisms that facilitate thumb flexion/extension and abduction/adduction,[10,11] as well as mechanisms focusing on thumb opposition/reposition rather than abduction/adduction.[12,13] Additionally, simpler one-DOF systems have been tested for their effectiveness in assisting thumb flexion and extension.[14,15]

In order to effectively use wearable hand robots in daily living, it is crucial to consider not only what the robots can do (functionality) but also how easy and user-friendly the robots are to operate (usability).[16] Recently, wearable robots made from soft materials have attracted attention from researchers due to their advantages of being compact, lightweight, comfortable, and free from concerns regarding misalignment.[17] To fully leverage the advantage of these devices, especially in terms of usability, researchers have also focused on using tendon-driven mechanisms due to their ability of reducing the complexity of the wearable parts (i.e., end-effector). Also, they have tried to reduce the number of actuators to make the actuation system compact and light. For instance, a differential mechanism for adaptive grasping,[14] a synergy-based actuation,[18] and a sequentially actuating mechanism[19,20] have been proposed to generate finger motions with fewer actuators. While previously developed mechanisms have contributed to reducing the number of actuators, they were primarily designed to focus on the enclosing phase. To grasp objects in various postures without increasing the number of actuators, a mechanism that considers the multi-DOF motion of the thumb and pre-shaping phase is needed.

In this article, we propose a soft wearable hand robot, Exo-Glove Poly III (EGP III) (Fig. 2), capable of assisting two different grasping strategies with a single actuator by using a slack-based sequential mechanism (SSM) (Supplementary Video S1). This mechanism enables the EGP III to assist both pre-shaping and enclosing phases of grasping. While the previous version, EGP II,[21] improved the usability (of EGP) and could grasp the object securely, it lacked thumb motions and could only realize a limited number of grasp postures. Our new design overcomes these limitations by designing a thumb module (TM) and developing the SSM to generate finger motions while using a single actuator. By doing so, the whole system could be designed to be fully wearable, including the electronic circuits. The performance of the system was evaluated with a healthy subject, demonstrating its ability to successfully perform daily tasks using various grasping strategies.

Glove Design

The EGP III is designed based on the EGP II but features significant advancements.[21] Unlike the EGP II, the wearable part of the EGP III consists of a main glove (MG) and a TM (Fig. 3a and c) that replaces the passive thumb structure. In addition to the wearable components, the system comprises a remote controller that detects the user's intended grasping strategy with buttons (Fig. 2c) and an actuation system (SSA) (Fig. 2a and b). This section details the glove design of EGP III, focusing on the advancements and modifications from EGP II.

Thumb module

The TM is designed to actively assist the thumb motions during the pre-shaping phase and the enclosing phase. Three
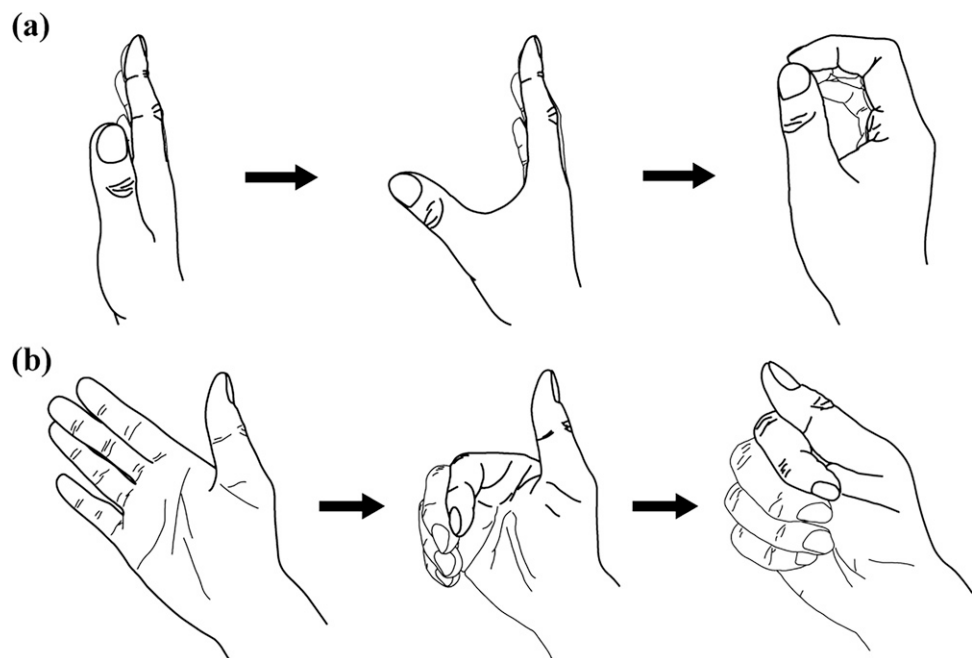

FIG. 1. Schematic of the hand posture according to the thumb motion. (a) Grasping with the abducted thumb. (b) Grasping with the adducted thumb.
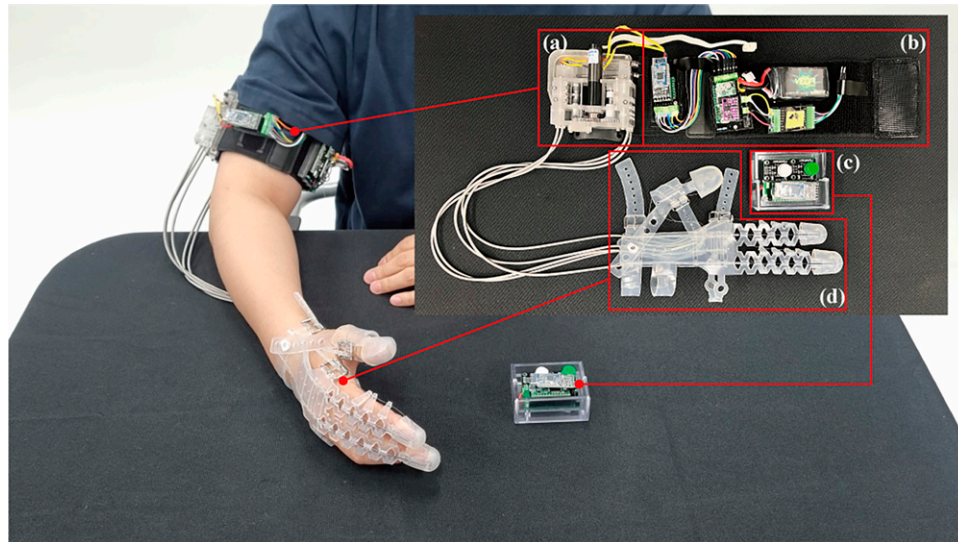
FIG. 2. Overview of the system worn by the human. **(a)** The SSA is bolted to a plastic part of a commercial armband. **(b)** Electronic circuits and a battery are attached to the armband using velcros. A bluetooth module is on the board and receives actuation signal from a remote controller. **(c)** Remote controller. *Green button*: abducted thumb grasping strategy. *White button*: adducted grasping strategy. When the button is pressed, the motor rotates, and when the button is not pressed, the motor maintains its current position. **(d)** Wearable part of the EGP III.

thumb motions are selected to be realized: the opposition for pre-shaping, and the flexion and the adduction for enclosing. Unlike the index and middle fingers, the thumb requires more complex motions during each phase. Unlike flexion, which can be assumed to be a planar motion, the thumb opposition, one of the essential thumb motions, is a three-dimensional motion.[22] Therefore, the TM surrounds and tightens the entire thumb so that it does not slip off even when tension is applied. The TM has an elastic band (EB) that enables the thumb reposition (reverse motion of the opposition) and the extension (Fig. 3c and d). In other words, when the motor releases the tendon, the EB pulls the thumb to go back to the initial position. The arrangement of the EB is inspired by the muscles in the dorsal side of the hand: the first dorsal interossei and the extensor pollicis longus. Since EB has to play the roles of both muscles, it originates from the lower center of the TM and is connected to the dorsal part of the MG using the connector.

Main glove

The MG follows the design of the EGP II, while tendon routing for the thumb motions and the passive elements are added. To reduce the number of actuators, passive extensors are used to make the initial hand posture open (Fig. 3c and d). Additional details are illustrated in Note S1, Supplementary Data.

Tendon routing

Tendon routings for thumb motions are developed and embedded in the MG and the TM. All routings form a loop, which reduces the deformation of the body compared with a routing that inserts the tendon into the body and ties it without shaping a loop. The opposer moves the thumb to the opposite side of the index and middle fingers, inspired by the opponens pollicis. Its pulley location is around the flexor carpi ulnaris, inspired by tendon transfer surgery.[23] This
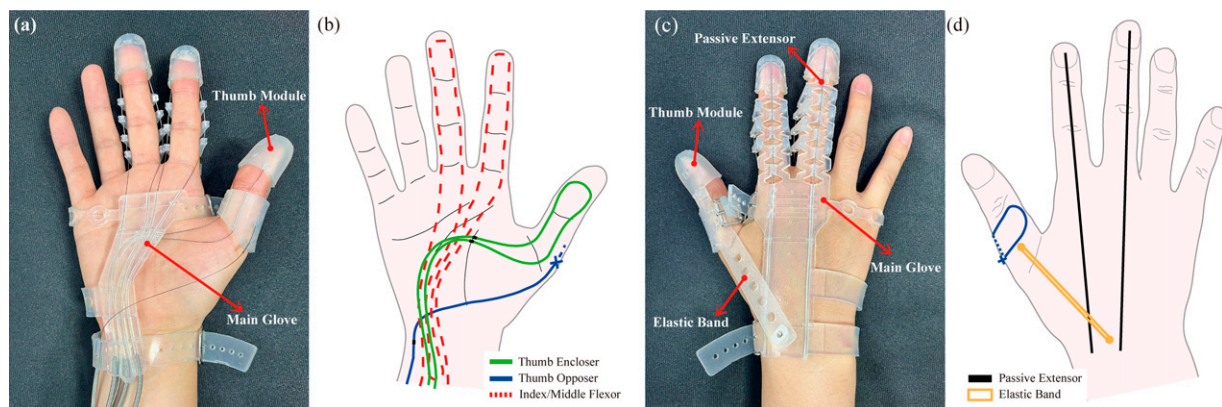

FIG. 3. Design overview of EGP III. **(a)** Palmar view. **(b)** Schematic of the tendon routings on palmar view. Black dots on the thumb encloser and the thumb opposer are pulley locations. "X" on the thumb opposer indicates a knot tying wrapped wire. **(c)** Dorsal view. **(d)** Schematic of the tendon routing and passive elements on dorsal view.

facilitates the thumb abduction and creates a larger hand aperture for grasping larger objects. The opposer wraps around the proximal phalanx and then passes through the pulley location (Fig. 3b and d).

For the enclosing phase, the thumb encloser is designed to move the thumb toward the other fingers, regardless of the position of the thumb. To achieve this, the encloser is designed to combine the adductor pollicis and flexor pollicis longus in the human hand. The pulley is placed in the middle of the palm to move the thumb toward the fingers and reduce the space between them in both the opposed and non-opposed positions (Fig. 3b).

Slack-Based Sequential Actuator

Tendon slack can delay the response time in tendon-driven systems.[24] Previous research has utilized tendon slack to modulate damper engagement in legged robots.[25] However, in tendon-driven systems with spools, slack can cause tendon derailment and system failure. To address this, In et al. developed a slack-enabling mechanism to remove slack around the spool.[26] Given that, we developed the SSM which uses the slack of the tendon as a key element for adjusting actuation timing for the spool-based tendon-driven

mechanism. Based on the previous study,[8] two grasping strategies are chosen to be implemented using the SSA: the abducted grasping strategy (AbTGS) and the adducted grasping strategy (AdTGS) (Note S3, Supplementary Data).

Principle of the mechanism

A sequence generation by the SSM is inspired by the tendon-driven mechanism, where actuator power is transmitted to the end-effector via tension. Tension is generated when the tendon slack is removed, initiating actuation. We devised a coupling method among multiple tendons with varying slack lengths, allowing the actuation timing of each tendon to be controlled by adjusting its slack length.

Figure 4 shows the principle of the SSM with a single spool and two tendons. Each end of the two different tendons (A, B) is connected to the same spool in a different section with a different slack length (Fig. 4a), where tendon A has a longer slack than tendon B. When the spool rotates to wind both tendons, the slacks of both tendons start to be removed. When slack B is removed, the actuation by tendon B starts while the tendon A is still loose without tension (Fig. 4b). After the spool winds the tendons more, slack A is removed, and the actuation by tendon A starts (Fig. 4c) while the
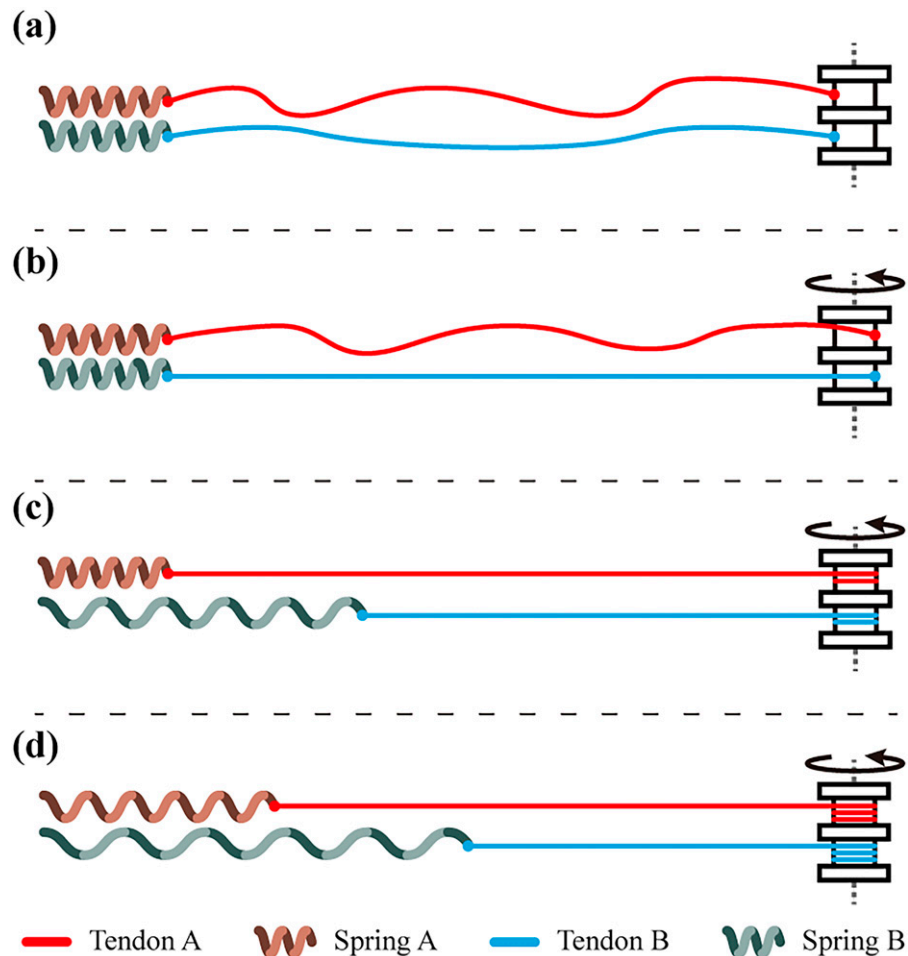

FIG. 4. Schematic of the principle of the slack-based sequential mechanism. Springs represent the end-effectors, where spring elongation means the end-effector is actuated. Slack length: **(a)** A > B. **(b)** A > B = 0. **(c, d)** A, B = 0. **(a)**, **(b)**, **(c)**, and **(d)** are in time order.

actuation by tendon B continues. A detailed explanation is provided in Note S4, Supplementary Data.

Actuator design

Based on the SSM and two grasping strategies, we designed the slack-based sequential actuator (SSA), combining tendons to achieve motion sequences for each strategy. One end of the thumb opposer is connected to the end-effector, while the other end is connected to the spool. Unlike the opposer, the flexor and the encloser have one end connected to the spool and the opposite end to the slack length adjusting section (Fig. 5b). These tendons shape a loop in each end-effector to transmit the power from the actuator (Fig. 5c).

The driving section (Fig. 5a) is designed to pull tendons simultaneously with a main motor, where it can realize AbTGS when rotating counterclockwise and AdTGS when rotating clockwise (Fig. 6a and b). The main motor is connected to the two spools via gears. The thumb opposer is tied to a spool, and the flexor and the thumb encloser are tied to the other spool in a different section. To utilize both directions of the rotation, a miniature motor-based slack-enabling mechanism is used to remove slack near the spool of the flexor and the encloser (Note S2, Supplementary Data).

One of the critical aspects in implementing grasping strategies into the SSA using SSM is the thumb opposition. As shown in Note S3, Supplementary Data, the thumb opposition occurs first, and the flexion of the index and the middle finger follows when realizing the AbTGS. Since the extent of the realized thumb opposition affects the hand aperture size, it should be considered when designing the driving

section of the SSA. The relationship among the extent of each motion is shown in the following equations:

$$L_1 = n_1 r_1 (\theta_3 - \theta_0) \tag{1}$$

$$L_2 = n_2 r_2 (\theta_3 - \theta_1) \tag{2}$$

$$L_1^* = n_1 r_1 (\theta_1 - \theta_0) \tag{3}$$

$$L_1^* = L_1 - \frac{n_1 r_1}{n_2 r_2} L_2 \tag{4}$$

$$= L_1 - \frac{v_1}{v_2} L_2 \tag{5}$$

L_1 represents the required total tendon length to achieve the full range of motion (stroke length) of the thumb opposition, and L_2 represents the stroke length of the flexion of the index and middle fingers. n_i ($i = 1, 2$) represents the angular velocity ratio of each spool to the motor, r_i ($i = 1, 2$) denotes the radius of each spool, and v_i ($i = 1, 2$) is the speed of each tendon (1: opposer, 2: flexor and encloser). θ is the angle spanned by the motor (Fig. 6). When the opposer is pulled about L_1^*, the flexor is started to be pulled. In other words, the slack of the flexor is removed at that time. Since L_1 and L_2 are determined based on the user's physical characteristics, L_1^* can be designed by modulating the speed ratio ($\frac{v_1}{v_2}$). Additionally, as the speed ratio decreases, the L_1^* increases, leading to the larger hand aperture. In this work, the speed ratio was designed to be minimized within the limited size of the actuator by adjusting the gear combination and the spool radius, resulting in a value of 0.065 (Note S5, Supplementary Data).
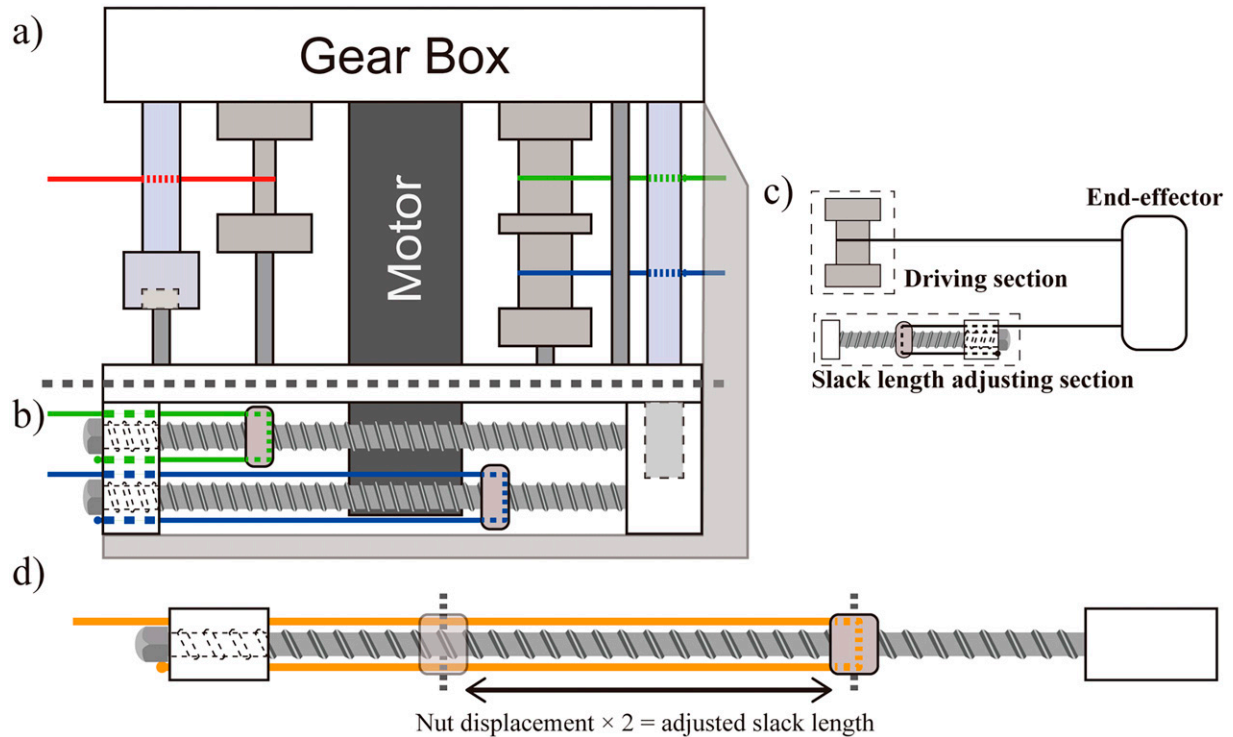

FIG. 5. Design of the slack-based sequential actuator. **(a)** Driving section of the actuator. **(b)** Slack length adjusting section of the actuator. *Gray* area of **(a)** and **(b)** is for the slack storage. **(c)** Schematic of the tendon (the flexor and the encloser) and the system. One end of the tendon is connected to the spool, and the tendon passes through the end-effector. The other end is connected to the slack length adjusting section. **(d)** Schematic of adjusting slack length.

FIG. 6. Schematic of motion sequence and pulled length of each tendon length. Topp represents the thumb opposer, Tenc represents the thumb encloser, and I/M_{fl} represents the index and middle finger flexor. *Dotted lines* in each tendon represent the corresponding tendon slack. θ_i ($0 \leq i \leq 6$) represents the rotation angle of the main motor at each timing. **(a)** Schematic of pulling tendon with the SSA to realize each grasping strategy. Spring A represents thumb opposition, Spring B represents index and middle finger flexion, and Spring C represents thumb enclosing. **(b)** Sequence of the tendon to be pulled according to the motor rotation. **(c)** Pulled length of tendons at each timing (*Dashed-lines* link each timing to its corresponding point in **(b)**). S_i ($i = 2, 3$) represents the slack length of the corresponding tendon. L_i ($i = 1, 2, 3$) represents the stroke length of the corresponding tendon. L_1^* represents the amount of pulled length of the Topp when the I/M_{fl} starts to be pulled.
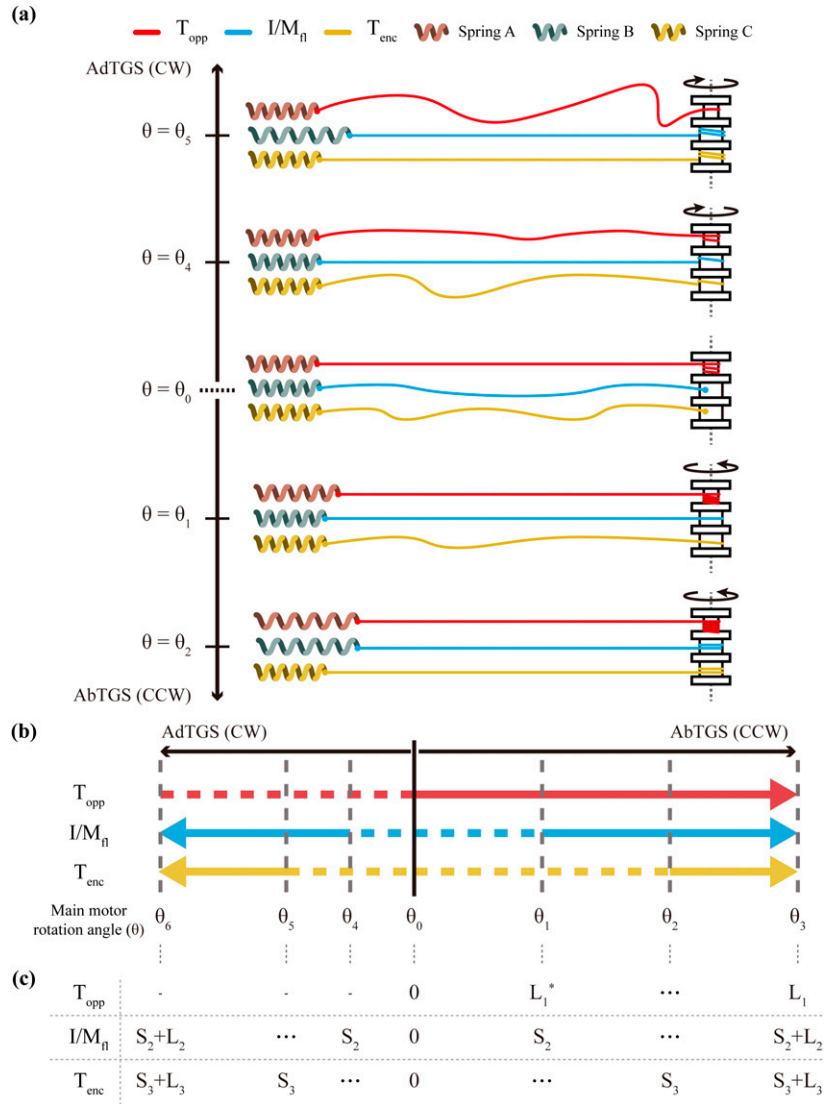

Since the thumb opposition is not involved in the AdTGS, the opposer is tied to the spool in a way that it is always released when the motor rotates clockwise. Unlike the AbTGS, since the stroke length of the encloser is shorter than L_2, the same driving speed can be used without adjustment, only utilizing slack to implement the grasping strategy.

In order to compensate for errors that can occur during the initial slack length setting due to the overlapped tendon on the spool and inaccuracy from knot-tying, the slack length adjusting section is designed in the actuator. In the slack length adjusting section (Fig. 5b and d), a screw mechanism is used for manual adjustment of the slack length and avoiding slack length change during actuation

FIG. 7. Schematic and results for the experiments of thumb motion tracking: **(c–e)** pulling the thumb opposer; **(f–h)** pulling the thumb encloser when the thumb is in the opposed state; **(i–k)** pulling the thumb encloser when the thumb is in the adducted state. The hand aperture size (*green arrow* in **(a)** and **(b)**) represents the amount of space the robot can create for the object and is calculated based on the distance between the thumb and the index finger (Note S7, Supplementary Data). Ab represents abduction angle, Ex represents extension angle, and Fl represents flexion angle. **(a)** Schematic of the hand aperture for the thumb opposition and the adduction. **(b)** Schematic of the hand aperture for the thumb flexion. **(c)** Schematic of the thumb motion while pulling the opposer. **(d)** The hand aperture size increases while realizing the thumb opposition. **(e)** Measured joint angles during the thumb opposition show that while the thumb opposition is being realized, the extension and abduction of the MCP joint occurs due to the EB. **(f)** Schematic of the thumb motion, pulling the encloser while the thumb is in an opposed state. **(g)** The hand aperture size decreases due to the adduction of the thumb. **(h)** The adduction and flexion of both the MCP and CMC joints are the dominant motions during the pulling of the encloser tendon when the thumb is in the opposed state. **(i)** Schematic of the thumb motion, pulling the encloser while the thumb is in the adducted state. **(j)** The hand aperture size decreases due to the flexion of the thumb. **(k)** The IP joint mainly flexes during the actuation, while other joints show slight movements due to the EB. IP joint follows the left axis. EB, elastic band.

(Note S6, Supplementary Data). A 50 mm commercial M2 bolt (stainless steel) is used as a screw, and a 3D-printed structure (Polylactic acid) is used as a nut. When the actuator does not operate the system, it is easy to move the screw to adjust the slack length because there is no tension in the tendon. Moving the nut to change the slack length and geometric constraint for the screw is shown in Supplementary Videos S2.
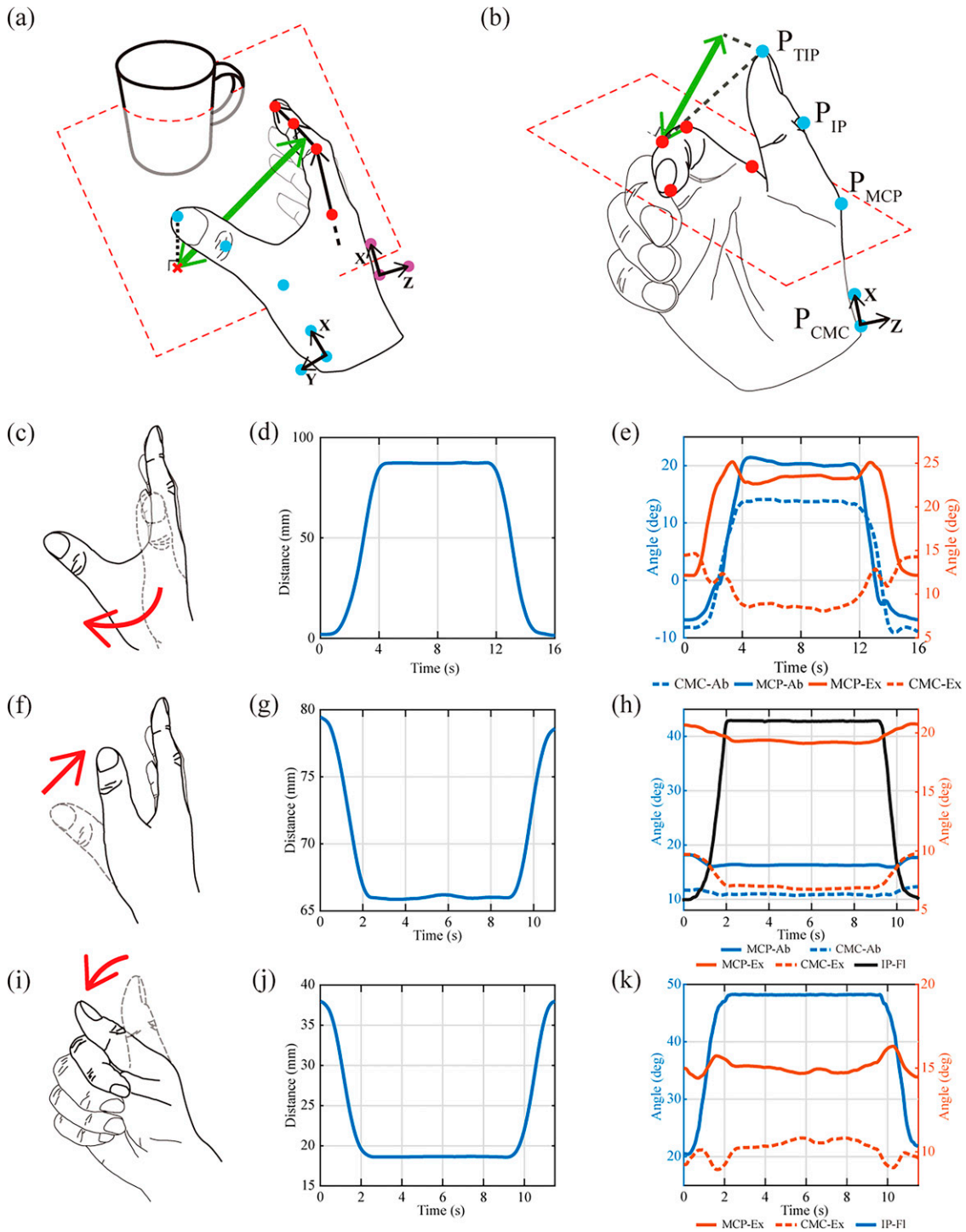
The proposed mechanism enables two grasping strategies with a single motor but results in slack extending outside the actuator, posing a risk of getting caught on something or malfunctioning. To prevent this, a slack storage is designed near the slack's emergence, separating it from the exterior to ensure reliable operation (Fig. 5a and b).

Experiment and Result

The proposed robot design and the concept of the mechanism were experimentally evaluated through a case study with a healthy subject (28 years old). During the experiments, the participant was instructed to use the unequipped hand to hold the equipped arm, preventing it from moving, while fully relaxing the equipped arm. The experimental procedures were approved by the Institutional Review Board of Seoul National University (IRB No. 2311/004-003). Referring to previous research,[27] motions and hand aperture size (Fig. 7a and b) are measured using a motion capture system (Note S7, Supplementary Data). In addition to the experiments for motion generation with the EGP III, a repeated experiment was conducted to verify the consistency of the actuation timing difference (Note S8, Supplementary Data), and grip strength was measured (Note S9, Supplementary Data).

Performance of the tendon routing of the TM

We validated the performance of the tendon routing in the TM by pulling each tendon with a slider-tendon linear actuator.[28] Considering the grasping strategies, experiments were conducted in three cases: the thumb opposition (Fig. 7c–e), thumb enclosing when the thumb is opposed (Fig. 7f–h), and thumb enclosing when the thumb is not opposed (Fig. 7i–k).

For the first case, the opposer applied force to the side of the thumb's proximal bone, directing it toward the pulley location. As a result, the carpometacarpal (CMC) joint abducted and flexed, realizing the thumb opposition (Fig. 7e), and the metacarpophalangeal (MCP) joint also abducted to go far away from the other fingers. While the thumb opposition was being realized, the EB kept applying force to extend and adduct the thumb. The force to adduct the thumb was compensated by the tension of the opposer, and the force to extend the thumb results in the extension of the MCP joint, which leads to enlarging the hand aperture size (Fig. 7d and e).

The next experiment is conducted with the thumb fixed on the opposite side of the other fingers (Fig. 7f). Pulling the encloser when the thumb is opposed causes the thumb to be adducted and flexed. Since the opposer remained fixed while the encloser was being pulled, the adduction angle and the flexion angle of the thumb were slightly changed (Fig. 7h). However, the reduction in hand aperture size indicates that the thumb was moving toward the index finger (Fig. 7g). This means that pulling the thumb encloser, when the thumb was in the opposed position, enabled the thumb to move toward the index and the middle fingers and push the object inside the hand.

Lastly, the encloser was pulled with the adducted thumb and the flexed index and middle fingers to form a space between the thumb and the index finger (Fig. 7i). Since the EB kept applying force to the thumb to extend, the flexion of the interphalangeal (IP) and the CMC joint, and the slight extension of the MCP joint occur (Fig. 7k). After the distal phalanx of the thumb and index finger contacted, the tendency of the motion reverses except for the IP joint. As the thumb flexes, the hand aperture size reduces, but due to the thickness of the glove, the calculated size did not reach zero (Fig. 7j).

Motion generation with different sequences by SSA

We conducted experiments to validate whether the actuator, designed based on the proposed mechanism and grasping strategies, realizes the necessary motions at different timings for each strategy. Since an increase in the tension means that the corresponding motion starts, we measured the tension of tendons for each motion to verify whether the motions start in the proper sequences. Additionally, by measuring the size of the hand aperture, we confirmed that space within the hand for the target object is formed during the realization of grasping strategies and that the fingers move to reduce the space and grasp the object. Each joint angle was measured during the experiment, following the calculation method used in a previous experiment (Note S7, Supplementary Data), to verify if the intended motions were generated. The slack lengths of the tendons were initially set based on the parameters established during the design process and the measured stroke lengths for each motion (Table 1). The experiment, where the slack lengths of the tendons are both zero, was also conducted to verify the performance of the mechanism (Note S10, Supplementary Data).

By rotating the main motor in the counterclockwise direction to realize the AbTGS, tensions increased in the order of the opposer, the flexor, and the encloser (Fig. 8d). Due to the counterclockwise rotation of the motor, the rotation angle of the motor is indicated as a negative value (Fig. 8c). While realizing the thumb opposition, the aperture size gradually increased even when the flexor began to be pulled, and then it started to decrease about one second later (Fig. 8b). The reason why the size did not decrease right after the flexor tension increased is that a certain level of tension is needed to overcome the restoring force of the passive extensors and flex the fingers. During the experiment, flexion of the MCP was generated (Fig. 8e) after the thumb encloser activated because the insertion point (to the TM) of the thumb encloser is above the MCP joint, and the tendon is trying to pull down the thumb toward its pulley location (Fig. 3). However, the EB of the TM was able to prevent full flexion. When the flexion of the index/middle fingers started, the aperture size started to decrease. When the motor stopped and the AbTGS stopped, the thumb, index, and middle fingers were gathered at one point (Fig. 8a).

TABLE 1. MEASURED STROKE LENGTH OF EACH MOTION

	Thumb opposer (L_1)	Index/middle flexor (L_2)	Thumb encloser
Stroke length (mm)	65.18	149.54	88.32

The subject wore the glove, and the STLA pulled each tendon 10 times for the measurement.[28] Measured lengths were averaged and presented in the table.
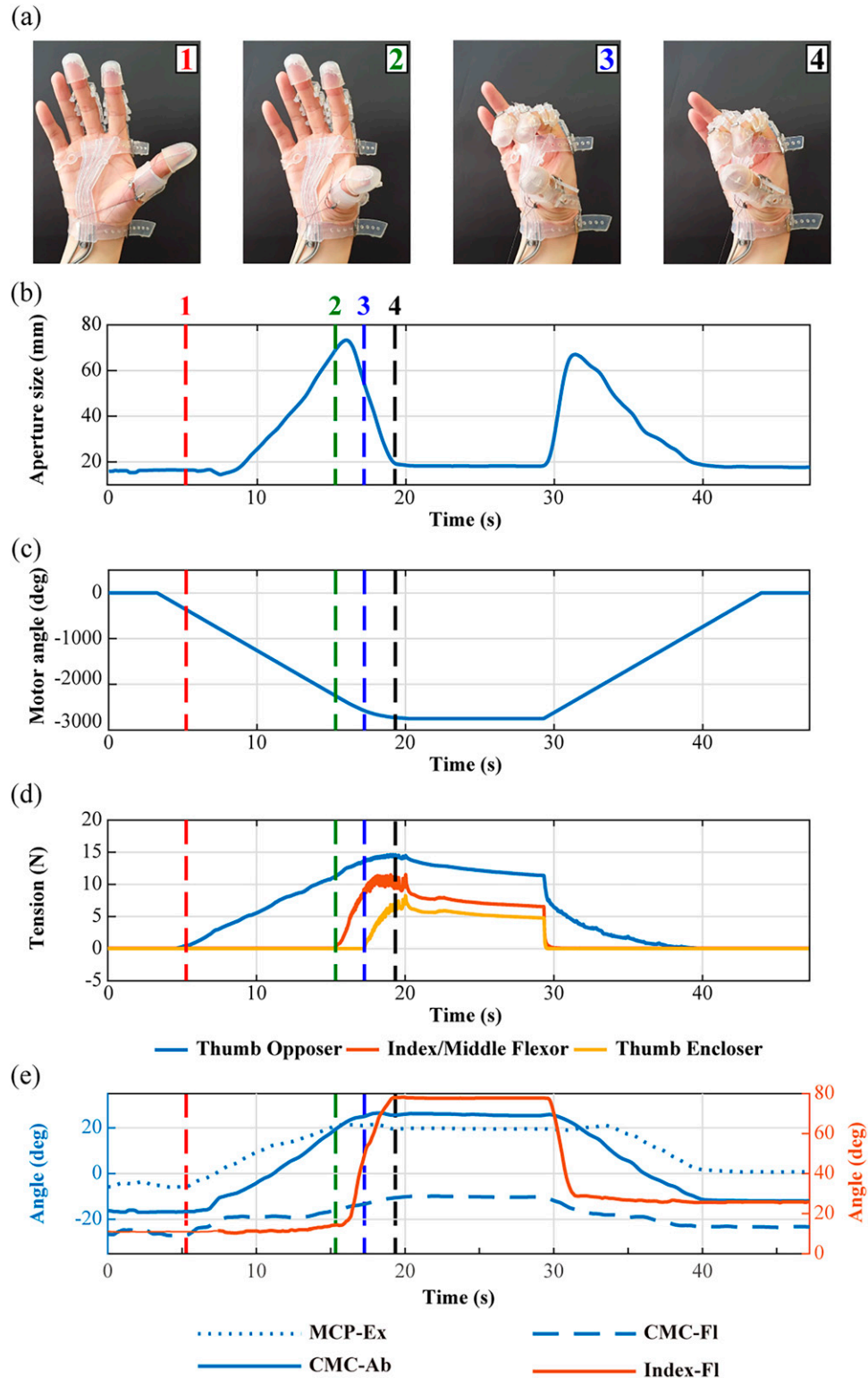
STLA, slider-tendon linear actuator.

FIG. 8. Experimental results for realizing AbTGS using the SSA. Opposition of the thumb occurred first, followed by the flexion of the index finger, and then the adduction and flexion of the thumb. (**a**) Photographs of the hand posture at four-time frames. The number and color of each label in the photo correspond to the number and the color of the dashed line in the graph. (**b**) Hand aperture size according to the time. After the index finger began to flex, the hand aperture size started to decrease. (**c**) Angle spanned by the motor while performing AbTGS, where the negative value comes from the counterclockwise rotation of the motor. (**d**) Tension of tendons. (**e**) Measured joint angle during the experiment. Ex and Ab denote extension and abduction, respectively. AbTGS, abducted grasping strategy.
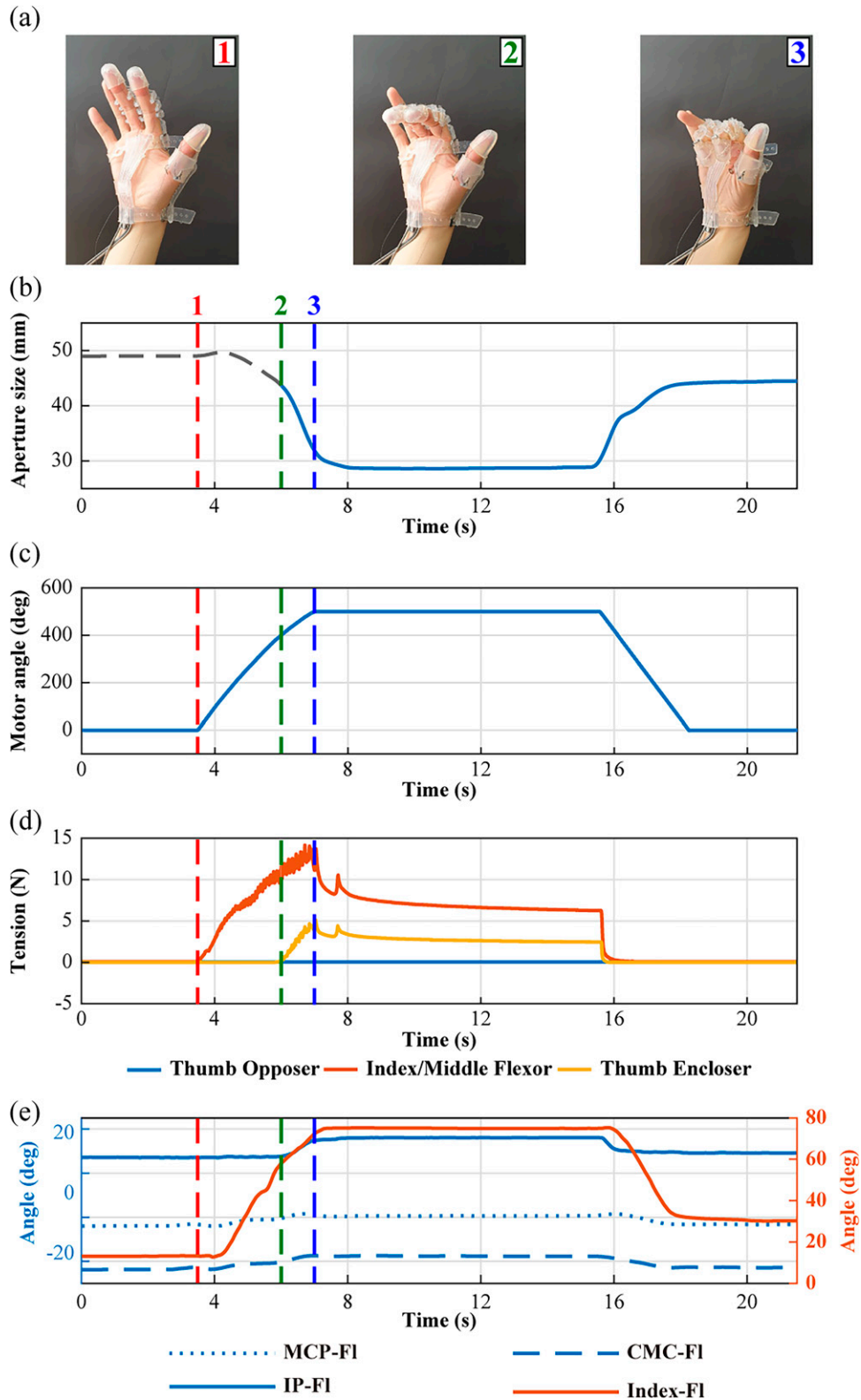
FIG. 9. Experimental results for AdTGS using the SSA. Flexion of the index finger occurred first, followed by the flexion of the thumb. **(a)** Photographs of the hand posture at three-time frames. The number and color of each label in the photo correspond to the number and the color of the *dashed line* in the graph. **(b)** Hand aperture size according to the time. Since the hand aperture is not formed until the index finger has flexed sufficiently (2), the line is shown in *gray* and marked with a *dashed* style before the sufficient flexion is achieved. **(c)** Angle spanned by the motor while performing AdTGS, where the positive value comes from the clockwise rotation of the motor. **(d)** Tension of tendons. **(e)** Measured joint angle during the experiment. Fl and Ab denote flexion and abduction, respectively. AdTGS, adducted grasping strategy.

FIG. 10. Photographs demonstrating the subject grasping daily objects with EGP III. **(a–d)** Each grasp posture (in each legend) is classified according to the grasp taxonomy.[8] Grasping a pen, a spoon, a bottle, and a plum (mockup). The left column shows results with the AbTGS, and the right column shows results with the AdTGS. **(e–k)** The name of the grasp posture is referred from a previously reported categorization.[29] Grasping a paper cup with a cylindrical grasp (Cyl), a candy with a pinch grasp (Pinch), grasping a pen with special pinch (SpP), grasping an iron with an oblique palmar grasp (Obl), grasping a mug with a hook grasp (Hook), grasping a book with a lumbrical grasp (Lum), and grasping a key with a lateral pinch (LatP).

Contrary to the AbTGS, rotating the motor in the clockwise direction realized the AdTGS (Fig. 9). During the AdTGS, the tension of the opposer did not increase because it was being released from the spool. The flexor and the encloser were being wound on the spool in the opposite direction to the AbTGS, and their tension increased to generate motions. The tension increased first in the flexor and then in the encloser. Since the space for the object is generated when the index finger is flexed enough, the hand aperture size before the encloser tension increases is indicated as the gray dashed line. When the encloser started to pull the thumb, the flexion angles of the IP, MCP, and CMC joints of the thumb increased, resulting in a reduction of the hand aperture size (Fig. 9e). As seen in Figure 9a, when the motor stopped after realizing AdTGS, the fingers formed a lateral grasp posture, enabling the hand to grip an object with the thumb in an adducted position.

Grasping various objects

In this experiment, the subject was instructed to grasp objects to evaluate the system performance in two areas: employing different grasping strategies and achieving common postures used in daily tasks. The subject wore the portable version of the system (Fig. 2) and was instructed to press the button until the object was grasped, based on the subject's judgment.

The subject was instructed to grasp four objects: (1) a pen, (2) a bottle, (3) a plum (mockup), and (4) a spoon (Fig. 10a–d). These four objects were selected from those commonly used in daily living. The first two objects were selected to represent cylindrical objects with different radii. The third object was selected to represent spherical objects, and the last one represents thin objects. In daily living, the objects are generally grasped and used with appropriate posture, based on human intention and the specific purpose of each object. For instance, the first three objects are usually grasped using the tripod grasp, wrap grasp, and sphere 3-finger, respectively, which are the result of the AbTGS. Furthermore, the last object is usually grasped using the lateral grasp which is the result of the AdTGS. Since the robotic system can assist with both AbTGS and AdTGS, the subject was instructed to use both strategies for each object to demonstrate the performance of the system. As shown in Figure 10, all of the objects were successfully grasped using both grasping strategies, and the final grasp posture is written in each figure.

In addition to the four objects, the subject was instructed to grasp seven objects: a cup, a candy, a pen, an iron, a mug, a book, and a key (Fig. 10e–k). The objects were selected to validate whether the system can grasp each object with proper common grasp postures. Based on the categorized common grasps for daily living,[29] 87.5% of the postures can be achieved by the system (Note S11, Supplementary Data).

Conclusion

This article proposes a wearable hand robot that is designed considering both functionality and usability. The system enables two different grasping strategies with a single actuator. To achieve this, the SSM is proposed, where the slack length is set differently for each tendon and tendons are pulled simultaneously. Based on the proposed mechanism and grasping strategies, the SSA was designed, including a slack length adjusting section to compensate for potential errors in the initial slack length setting. Experiments validated the performance of both the glove and the actuator, confirming their ability to grasp a variety of objects. The proposed mechanism is expected to simplify the actuation systems of wearable robots, not limited to the hand but also potentially aiding in walking or upper limb movements.

Although the ability of the system to grasp various objects using two strategies was validated, further studies are needed in future. Due to the characteristics of the proposed mechanism, motions are preprogrammed and end simultaneously, requiring design optimization that considers factors like slack length, total actuation time, and the timing of motions. Additionally, the passive elements designed to return the fingers to an open hand may struggle to fully extend the fingers after repeated use due to the friction and the human joint properties (especially for stroke patients). Increasing the stiffness of the passive elements could enable the full extension, but this may affect the intended trajectory of the fingers during grasping, indicating a need for further research on passive elements. In future studies, because the system was tested only on a healthy subject, further clinical trials should be carried out with individuals who cannot use their hands.

Author Disclosure Statement

No competing financial interests exist.

Authors' Contributions

Conceptualization: K.B.K., H.C., B.B.K. and K.-J.C.; methodology: K.B.K., and H.C.; investigation: K.B.K., S.C., and H.C.; visualization: K.B.K., ,H.C., and B.K.; funding acquisition: K.-J.C.; project administration: K.B.K., and K.-J.C.; supervision: K.-J.C.; writing–original draft: K.B.K.; writing–review and editing: K.B.K., H.C., B.K., and K.-J.C.

Funding Information

Supplementary Material

Supplementary Data
Supplementary Video S1
Supplementary Video S2

References

1. Hoff B, Arbib MA. Models of trajectory formation and temporal interaction of reach and grasp. J Mot Behav 1993; 25(3):175–192.
2. Jeannerod M. The formation of finger grip during prehension. a cortically mediated visuomotor pattern. Behav Brain Res 1986;19(2):99–116.

3. Lin H-T, Kuo L-C, Liu H-Y, et al. The three-dimensional analysis of three thumb joints coordination in activities of daily living. Clin Biomech (Bristol) 2011;26(4):371–376.

4. Li Z-M, Tang J. Coordination of thumb joints during opposition. J Biomech 2007;40(3):502–510.

5. Paulignan Y, Frak V, Toni I, et al. Influence of object position and size on human prehension movements. Exp Brain Res 1997;114(2):226–234.

6. Cotugno G, Althoefer K, Nanayakkara T. The role of the thumb: Study of finger motion in grasping and reachability space in human and robotic hands. IEEE Trans Syst Man Cybern, Syst 2017;47(7):1061–1070.

7. Neumann DA, et al. "Kinesiology of the Musculoskeletal System," Mosby: St. Louis; 2002. pp. 25–40.

8. Feix T, Romero J, Schmiedmayer H-B, et al. The grasp taxonomy of human grasp types. IEEE Trans Human-Mach Syst 2016;46(1):66–77.

9. Suarez-Escobar M, Rendon-Velez E. An overview of robotic/mechanical devices for post-stroke thumb rehabilitation. Disabil Rehabil Assist Technol 2018;13(7):683–703.

10. Chen W, Li G, Li N, et al. Soft exoskeleton with fully actuated thumb movements for grasping assistance. IEEE Trans Robot 2022;38(4):2194–2207.

11. Tran P, Jeong S, Wolf SL, et al. Patient-specific, voice-controlled, robotic flexotendon glove-ii system for spinal cord injury. IEEE Robot Autom Lett 2020;5(2):898–905.

12. Kim DH, Park H-S. "Cable actuated dexterous (cadex) glove for effective rehabilitation of the hand for patients with neurological diseases," In 2018 IEEE/RSJ International Conference on Intelligent Robots and Systems (IROS), IEEE pp. 2305–2310, 2018.

13. Rose CG, O'Malley MK. Hybrid rigid-soft hand exoskeleton to assist functional dexterity. IEEE Robot Autom Lett 2019;4(1):73–80.

14. In H, Kang BB, Sin M, et al. Exo-glove: A wearable robot for the hand with a soft tendon routing system. IEEE Robot Automat Mag 2015;22(1):97–105.

15. Xiloyannis M, Cappello L, Binh KD, et al. Preliminary design and control of a soft exosuit for assisting elbow movements and hand grasping in activities of daily living. J Rehabil Assist Technol Eng 2017;4:2055668316680315.

16. Bützer T, Lambercy O, Arata J, et al. Fully wearable actuated soft exoskeleton for grasping assistance in everyday activities. Soft Robot 2021;8(2):128–143.

17. Nycz CJ, Bützer T, Lambercy O, et al. Design and characterization of a lightweight and fully portable remote actuation system for use with a hand exoskeleton. IEEE Robot Autom Lett 2016;1(2):976–983.

18. Xiloyannis M, Cappello L, Khanh DB, et al. and "Modelling and design of a synergy-based actuator for a tendon-driven soft robotic glove," In 2016 6th IEEE International Conference on Biomedical Robotics and Biomechatronics (BioRob), pp. 1213–1219, IEEE, 2016.

19. Park CB, Hwang JS, Gong HS, et al. A lightweight dynamic hand orthosis with sequential joint flexion movement for postoperative rehabilitation of flexor tendon repair surgery. IEEE Trans Neural Syst Rehabil Eng 2024; 32:994–1004.

20. Zhang Y, Zhang W, Yang J, et al. Bioinspired soft robotic fingers with sequential motion based on tendon-driven mechanisms. Soft Robot 2022;9(3):531–541.

21. Kang BB, Choi H, Lee H, et al. Exo-glove poly ii: A polymer-based soft wearable robot for the hand with a tendon-driven actuation system. Soft Robot 2019;6(2):214–227.

22. Hollister A, Giurintano DJ. Thumb movements, motions, and moments. J Hand Ther 1995;8(2):106–114.

23. Lee DH, Oakes JE, Ferlic RJ. Tendon transfers for thumb opposition: A biomechanical study of pulley location and two insertion sites. J Hand Surg Am 2003;28(6):1002–1008.

24. Muraoka T, Muramatsu T, Fukunaga T, et al. Influence of tendon slack on electromechanical delay in the human medial gastrocnemius in vivo. J Appl Physiol (1985) 2004; 96(2):540–544.

25. Mo A, Izzi F, Gönen EC, et al. Slack-based tunable damping leads to a trade-off between robustness and efficiency in legged locomotion. Sci Rep 2023;13(1):3290.

26. In H, Jeong U, Lee H, et al. A novel slack-enabling tendon drive that improves efficiency, size, and safety in soft wearable robots. IEEE/ASME Trans Mechatron 2017;22(1): 59–70. no

27. Kim DH, Lee Y, Park H-S. Bioinspired high-degrees of freedom soft robotic glove for restoring versatile and comfortable manipulation. Soft Robot 2022;9(4):734–744.

28. Kim B, Jeong U, Kang BB, et al. Slider-tendon linear actuator with under-actuation and fast-connection for soft wearable robots. IEEE/ASME Trans Mechatron 2021; 26(6):2932–2943. no

29. Vergara M, Sancho-Bru JL, Gracia-Ibáñez V, et al. An introductory study of common grasps used by adults during performance of activities of daily living. J Hand Ther 2014; 27(3):225–233; quiz 234.

Address correspondence to:
Kyu-Jin Cho
Biorobotics Laboratory
Department of Mechanical Engineering/Soft Robotics
Research Center/IAMD
Seoul National University
Gwanak-ro 1
Gwanak-gu, Seoul
Korea

E-mail: kjcho@snu.ac.kr